

^{99m}Tc -3PRGD₂ SPECT Predicts the Outcome of Endostar and Cisplatin Therapy in Xenograft Animals

Dose-Response:
An International Journal
October-December 2019:1-7
© The Author(s) 2019
Article reuse guidelines:
sagepub.com/journals-permissions
DOI: 10.1177/1559325819882544
journals.sagepub.com/home/dos



Wei Sun¹, Guifu He², Mingming Zhang³, Yi Zhao², Hongmei Yu⁴, Yi Li⁵, Wei Wu², and Tiefeng Ji⁶

Abstract

Aims: Our study was designed to investigate the usefulness of ^{99m}Tc -3PRGD₂ single-photon emission computed tomography (SPECT) for noninvasively monitoring the response of integrin $\alpha_v\beta_3$ expression to antiangiogenic treatment with endostar and cisplatin in xenograft animals.

Methods: ^{99m}Tc -3PRGD₂ SPECT imaging was performed at days 0, 7, 14, and 21. Tumors were harvested at all imaging time points for Western blotting and histopathological analysis.

Result: In ^{99m}Tc -3PRGD₂ SPECT imaging, the radioactivity accumulation of NaCl group rised gradually in the first half and dispersed on day 21 due to the necrosis of the tumor. While the radioactivity accumulation of treated groups gradually decreased throughout the course. The downtrend of tumor to nontumor ratio in endostar-treated group was more remarkable than cisplatin-treated group. The expression of intergrin $\alpha_v\beta_3$ of treated groups was lower than NaCl group from day 14. The expression of intergrin $\alpha_v\beta_3$ of endostar-treated group was significantly lower than cisplatin-treated group from baseline onward.

Conclusion: It's demonstrated that the ^{99m}Tc -3PRGD₂ could noninvasively visualize and semiquantify tumor angiogenesis in the xenograft model and monitor the response to the antiangiogenic therapy of endostar and cisplatin effectively. It also can predict the outcome of endostar and cisplatin therapy in xenograft animals.

Keywords

^{99m}Tc -3PRGD₂, antiangiogenic, endostar, cisplatin

Introduction

In recent 50 years, for a variety of reasons, lung cancer is the leading cause of cancer deaths worldwide,¹ which threatens many lives. Traditional chemotherapy plays an important role in the lung cancer treatment, but its overall effect is still not perfect.

Angiogenesis was associated with the growth and metastasis of lung cancer. Antiangiogenesis strategy became focus and development direction for the lung cancer treatment in recent years. Previous researches showed that inhibition of angiogenesis is a promising strategy for lung cancer and antiangiogenesis-targeted therapy plays an important role in strengthening chemotherapy efficacy and prolonging patient survival.^{2,3} However, these drugs are expensive and the outcomes came out slowly during the treatment due to the stability of the new vascular endothelial cells.

Imaging tools have been used to help diagnosing and monitoring cancer therapy for years.⁴⁻⁶ But traditional tools such as

¹ Institute of Pediatrics, First Hospital, Jilin University, Changchun, Jilin, China

² Department of Nuclear Medicine, Jilin Provincial Tumor Hospital, Changchun, Jilin, China

³ Department of Molecular Biology, College of Basic Medical Sciences, Jilin University, Changchun, Jilin, China

⁴ Department of Blood Transfusion, China-Japan Union Hospital, Jilin University, Changchun, Jilin, China

⁵ State Key Laboratory of Inorganic Synthesis and Preparative Chemistry, College of Chemistry, Jilin University, Changchun, Jilin, China

⁶ Department of Radiology, First Hospital, Jilin University, Changchun, Jilin, China

Received 4 May 2019; received revised 3 August 2019; accepted 11 August 2019

Corresponding Authors:

Tiefeng Ji, Department of Radiology, First Hospital, Jilin University, Changchun, Jilin 130021, China.

Email: jitiefeng460@163.com

Wei Wu, Department of Nuclear Medicine, Jilin Provincial Tumor Hospital, Changchun, Jilin 130021, China.

Email: goodwuwei@163.com



Creative Commons Non Commercial CC BY-NC: This article is distributed under the terms of the Creative Commons Attribution-NonCommercial 4.0 License (<http://www.creativecommons.org/licenses/by-nc/4.0/>) which permits non-commercial use, reproduction and distribution of the work without further permission provided the original work is attributed as specified on the SAGE and Open Access pages (<https://us.sagepub.com/en-us/nam/open-access-at-sage>).

X-ray and computed tomography (CT) are not desirable for antiangiogenic drugs due to relying on tumor volume change to evaluate the treatment effect.^{4,5} Therefore, it is hard to use traditional solid tumor evaluation methods to determine their efficacy. It is urgent to find a feasible method in evaluating the outcome of antiangiogenesis-targeted therapy for lung cancer. Molecular receptor imaging, basing on targeted combination between ligand and receptor, can help clinicians design individualized treatment to improve the outcome of lung cancer for its high sensitivity and specificity.⁷⁻⁹

Integrin $\alpha_v\beta_3$ is one type of integrins family, which is heterodimeric transmembrane receptor that mediates adhesion to the extracellular matrix. It has been found that integrin $\alpha_v\beta_3$, widely distributed in new blood vessels, has been documented as being associated with tumor angiogenesis and metastasis.⁵ Arg-Gly-Asp (RGD) peptides and analogs, novel $\alpha_v\beta_3$ -specific tracers, can specifically target the integrin $\alpha_v\beta_3$ receptor.^{6,10} Therefore, RGD radiolabeled by different nuclides has been intensively investigated for noninvasive functional imaging of tumors in preclinical and clinical studies. Such as, technetium-99 m radiolabeled RGD dimer (^{99m}Tc-HYNIC-3PEG₄-E[c(RGDfK)₂, ^{99m}Tc-3PRGD₂] single-photon emission computed tomography (SPECT) imaging can provide more accurate and timelier information than structural imaging alone.¹¹ Cisplatin is a broad-spectrum antitumor drug. It works by destroying the function of DNA and inhibiting mitosis in tumor cells and always used to treat a variety of cancers, including lung cancer.¹² And Endor is a targeted drug against tumor neovascularization. It inhibits tumor proliferation or metastasis by preventing the new blood vessels formation and blocking tumor nutrition supply.¹³

Therefore, we conducted this prospective study to determine the correlation between different tumor angiogenesis changes with the end-of-treatment response to determine whether ^{99m}Tc-3PRGD₂ SPECT can predict short-term outcomes of chemoradiotherapy plus bevacizumab in xenograft animals.

Materials and Methods

Antibodies and Regents

Goat serum (Abcam, Cambridge, Massachusetts), rat anti-integrin β_3 antibody (cat. no. 181720; BD Biosciences, Franklin Lakes, New Jersey), rat anti-CD31 antibody (1:100; cat. no. 551262; BD Biosciences), Cy3-conjugated goat anti-rat (1:100; cat. no. 115-165-003; Jackson ImmunoResearch Europe Ltd, Newmarket, the United Kingdom), goat anti-rat secondary antibodies (1:100; cat. no. 115-095-003; Jackson ImmunoResearch Europe Ltd), and glyceraldehyde phosphate dehydrogenase (GAPDH) were used as loading controls. The total protein level was normalized to the GAPDH protein level.

Treatment Protocol

All animal experiments were performed in accordance with the protocol approved by the Institutional Animal Care and Use

Committee at Jilin University (Changchun, China). Forty BALB/c xenograft mice (4-5 weeks, male and female half) with lung adenocarcinoma were chosen and divided into 3 groups: NaCl group (n = 12), cisplatin group (n = 14), and endostar group (n = 14). All the groups were size-matched, with an average tumor volume of $160 \pm 60 \text{ mm}^3$ 1 day before baseline SPECT imaging. Then, the mice in each group were injected on alternate days with saline solution (0.1 mL per mouse), cisplatin (5 mg/kg per mouse), and endostar (20 mg/kg per mouse).

Imaging Protocol

Six mice in each group were selected randomly for being administered with $\approx 300 \mu\text{Ci}$ of ^{99m}Tc radiotracer in 0.1 mL saline via tail vein injection. And then ^{99m}Tc-3PRGD₂ SPECT imaging and tumor measurement at baseline and days 7, 14, and 21 after treatment were performed. For semiquantitative analysis of tracer uptake in tumors following ^{99m}Tc-3PRGD₂ SPECT imaging, region of interests were drawn around the entire tumor and to the contralateral normal tissue with the same size of the tumor, and tumor to nontumor (T/N) ratios of ^{99m}Tc-3PRGD₂ SPECT were determined. And for tumor measurement, the tumor volume (mm^3) = $\pi/6 \times \text{length (mm)} \times \text{width (mm)} \times \text{height (mm)}$.

Western Blotting

Western blotting was performed in accordance with standard protocol. Briefly, the samples were lysed and denatured in $5 \times$ sample buffer. Same amounts of proteins were separated on a 10% sodium dodecyl sulfate-polyacrylamide gel and transferred to a nitrocellulose membrane. The nitrocellulose membrane was then incubated with 5% nonfat milk in Tris-buffered saline (150 mM NaCl, 20 mM Tris-HCl, pH7.4) with primary antibody at 4°C overnight. After washing, the membrane was further incubated with secondary antibody for 45 minutes and proteins were detected with an Electro-Chemi-Luminescence (Thermo Pierce, Rockford, USA) detection system. Image J software was used to measure the band intensity.

After the final acquisition of the scan, the animals were sacrificed, and the tumors were excised and fixed. Then, tumor inhibition rate were calculated.

Tumor Immunostaining

Immunofluorescence staining was performed to determine the location and expression of integrin $\alpha_v\beta_3$. Tumors were sectioned into 2 pieces for immunostaining and hematoxylin and eosin (H&E) staining. Once tumors were harvested, the tumor sections for immunostaining were immediately snap-frozen in optical cutting temperature solution (99% purity, Sigma-Aldrich, Saint Louis, USA; Merck KGaA, Darmstadt, Germany). Tumors were then cut into 5-mm sections. Following a thorough drying at room temperature, slides were fixed with ice-cold acetone for 10 minutes and then air dried for 20 minutes at room temperature. The sections were then blocked with 10% goat serum (Abcam) for 30 minutes at room temperature and then incubated

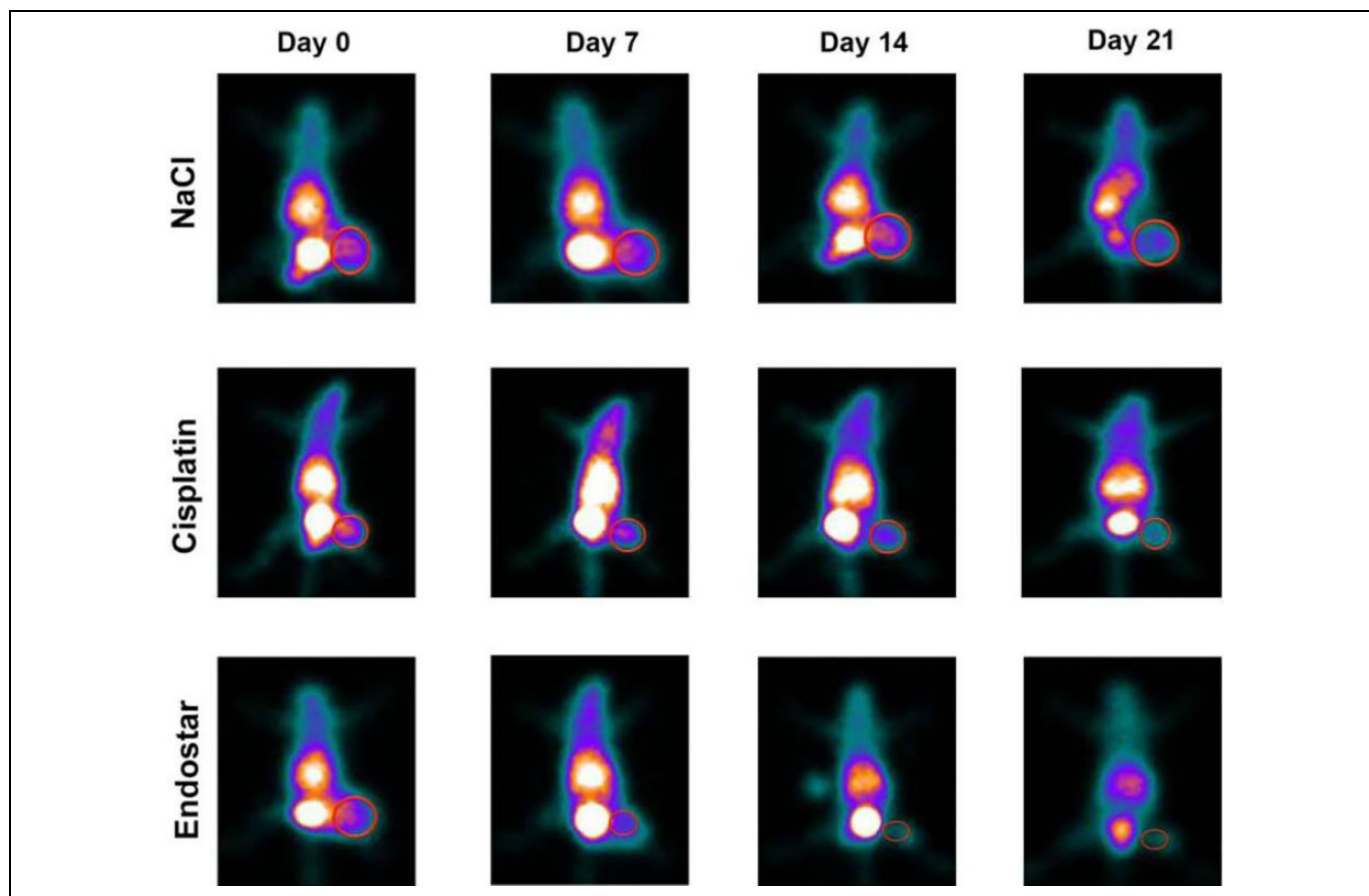


Figure 1. Single-photon emission computed tomography images demonstrating uptake of ^{99m}Tc -3PRGD₂. Representative SPECT images demonstrating uptake of ^{99m}Tc -3PRGD₂ in tumors of NaCl-treated, Cisplatin-treated and Endostar-treated animals for duration of study. ^{99m}Tc -3PRGD₂ retention in NaCl group tumor increased up to day 14 before decreasing slightly by day 21. Retention of ^{99m}Tc -3PRGD₂ in tumor (circled) of Cisplatin-treated animal decreased continuously and slowly. In comparison, Endostar-treated animal decreased significantly from day 3. Skeletal muscle, taken as reference tissue, showed no significant difference in ^{99m}Tc -3PRGD₂ retention among groups on each day. Excretion of ^{99m}Tc -3PRGD₂ was predominantly urinary.

with rat anti-integrin β_3 antibody (1:100; cat. no. 181720; BD Biosciences) and rat anti-CD31 antibody (1:100; cat. no. 551262; BD Biosciences) for 1 hour at room temperature. The β_3 antibody was chosen to represent $\alpha_v\beta_3$ as the only other integrin with a $\alpha\beta_3$ subunit besides $\alpha_v\beta_3$ is expressed on platelets. The majority of β_3 in the tumor sections is likely to be in the vasculature and tumor cells. After incubating with Cy3-conjugated goat anti-rat (1:100; cat. no. 115-165-003; Jackson ImmunoResearch Europe Ltd) and fluorescein isothiocyanate-conjugated goat anti-rat secondary antibodies (1:100; cat. no. 115-095-003; Jackson ImmunoResearch Europe Ltd) at room temperature (25°C) for 4 hours, the sections were washed with phosphate-buffered saline. Fluorescence was visualized with a Nikon fluorescence microscope at $\times 200$ magnification (Nikon Eclipse E600; Nikon Corporation, Tokyo, Japan).

H&E Staining

Histopathological analysis was performed by H&E staining of tumors. Briefly, all the tissues were fixed in 10% neutral-buffered formalin at room temperature (25°C) for 4 hours.

Tissues were embedded in paraffin and 4-mm sections were deparaffinized and rehydrated using a graded alcohol series. Sections were stained with H&E at room temperature (25°C) for 20 minutes to evaluate the morphology and then examined under a light microscope. Aperio's Image Scope v10.1.3.2028 Viewer (Leica Microsystems, GmbH, Wetzlar, Germany) was used to visualize the whole-slide digital scans and capture images in 30 fields of view for analysis.

Date Analysis

All data were expressed as the mean (standard deviation). Statistical analyses were performed using software Graph Pad Prism 5.0. $P < .05$ was considered to indicate statistical significance.

Results

Effect of Tumor Uptake After Treatment

The representative SPECT imaging of tumor-bearing mice 1 hour after injection of ^{99m}Tc -3PRGD₂ was shown in Figure 1.

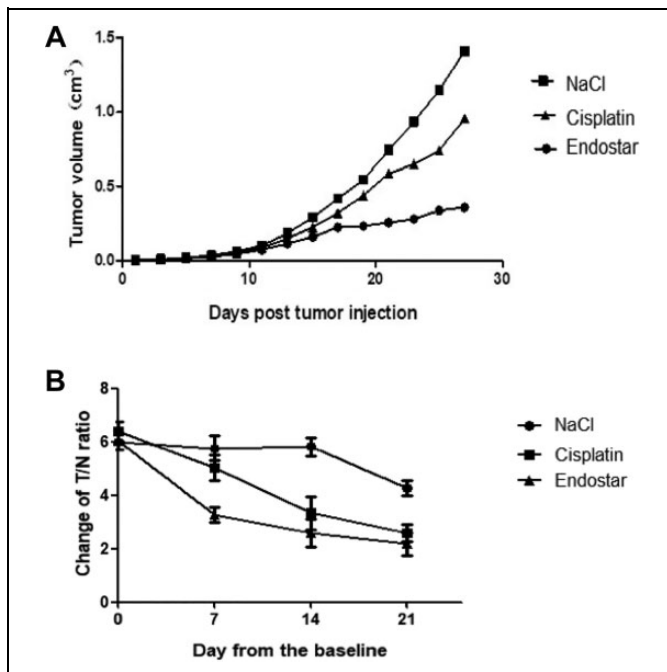


Figure 2. The effect of treatment on tumor retention. A, The change of tumor volumes of the control group and the treated groups. B, The change of T/N ratio of the control group and the treated groups (n = 3).

High radioactivity accumulation stood for high tumor uptake. The tumor could be clearly visualized with excellent contrast to contralateral background. As showed in Figure 1, the radioactivity accumulation of NaCl-treated group became more and more higher from baseline to day 14 and disperse on day 21 due to the necrosis of the tumor. On the contrary, the radioactivity accumulation of cisplatin- and endostar-treated groups both became lower. Moreover, the radioactivity accumulation of cisplatin treated was hardly detected on day 21, and the radioactivity accumulation of endostar treated was hardly detected on day 14.

Effect of Treatment on Tumor Retention

During the experiment, the sizes of the tumors were measured and the volumes of tumors were calculated. In day 28, the tumor volumes reached 210 and 230 mm³ for the treated group versus 320 mm³ for the NaCl group ($P < .05$). Besides, the average tumor inhibition rate was estimated by T/N ratios. As shown in Figure 2A, there is slightly significant difference of tumor volumes between NaCl group and cisplatin-treated group ($P < .05$), but there is highly significant difference between NaCl-treated group and endostar group ($P < .05$). In addition, visually, the T/N ratio change trend (Figure 2B) of the endostar-treated group declined sharply from baseline to day 7 and then decreased slowly to day 21; in comparison, the T/N ratio change trend of cisplatin-treated group declined equably from baseline to day 21 and those change trend in treated groups were significantly different from NaCl group ($P < .05$). The significant difference was not observed in the

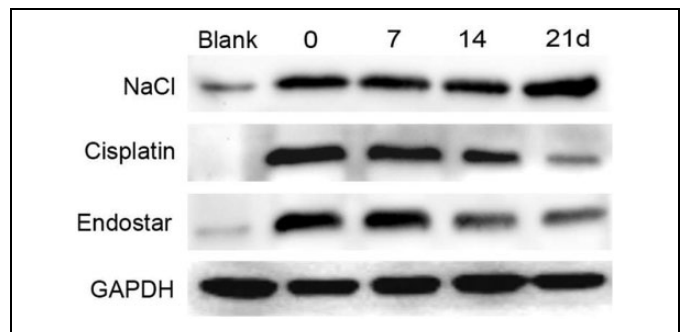


Figure 3. The $\alpha_v\beta_3$ protein expression detection by Western blot. The expression level of integrin $\alpha_v\beta_3$ under different groups of NaCl-treated, Cisplatin-treated and endostar-treated at each imaging point. The expression of integrin $\alpha_v\beta_3$ of Cisplatin-treated and Endostar-treated groups were lower than NaCl group from day 14. Especially, the expression of integrin $\alpha_v\beta_3$ of Endostar-treated group was significantly decreased from day 7 to 21. (n = 3).

baseline imaging among groups ($P > .05$). It was worth mentioning that no early resistance was found in our study and no observable body weight loss or any other side effects were observed during the treatment period, indicating that the dosage was safe.

For specificity analysis, skeletal muscle was chosen as a reference tissue, and no significant difference was demonstrated in muscle uptake before or after therapy. This result indicates that the decrease in tumor uptake observed with cisplatin and endostar therapy was specific.

Integrin $\alpha_v\beta_3$ Expression Validation

For the purpose of validation of integrin $\alpha_v\beta_3$ expression, we used the tumor tissue harvested at baseline and days 7, 14, and 21 to perform Western blotting, as shown in Figure 3. It was clearly showed that the expression of integrin $\alpha_v\beta_3$ of cisplatin- and endostar-treated groups were lower than NaCl group from day 14. Especially, the expression of integrin $\alpha_v\beta_3$ of endostar-treated group was significantly decreased from day 7 to 21. And the decrease level was more significant than the cisplatin-treated group.

Effect of Treatment on Survival Time

To investigate the effect of cisplatin and endostar in tumor-bearing mice, we made survival rate in Figure 4. In virtue of log-rank test, it showed that the difference between the NaCl group and the treated groups and between cisplatin- and endostar treated groups could prolong the survival rate significantly than the NaCl group (Figure 4A-C, $P < .05$). Moreover, the survival rate of endostar-treated group was much longer than cisplatin-treated group ($P < .05$).

Discussion

Angiogenesis plays important roles in various normal physiological processes and deregulation of angiogenesis has been

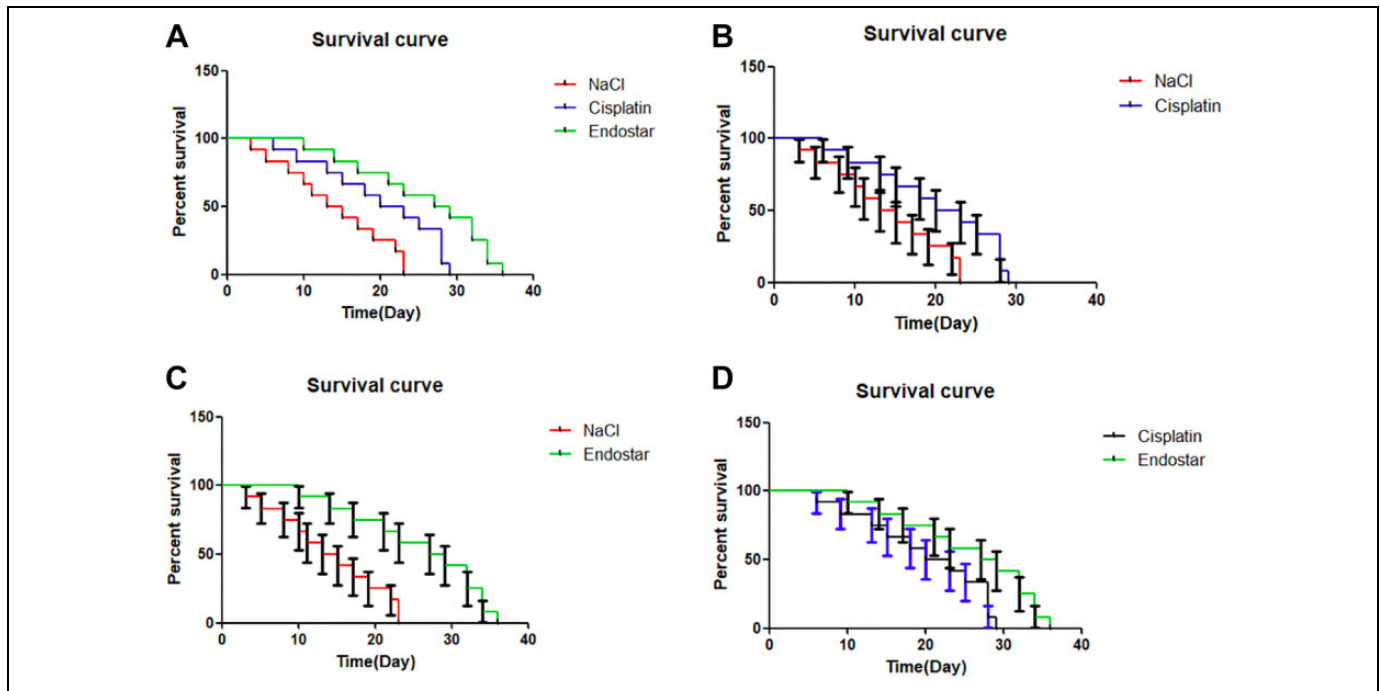


Figure 4. Survival status was analyzed by log-rank test. A, The difference between the NaCl group and the treated groups was significant ($P < .05$). B, The difference between the NaCl group and the Cisplatin-treated group was significant ($P < .05$). (C) The difference between the NaCl group and the Endostar-treated group was significant ($P < .05$). D, The difference between the Cisplatin-treated group and the Endostar-treated group was significant ($P < .05$; $n = 12$).

found in several pathological conditions and many human diseases.^{14,15} Moreover, angiogenesis is essential for tumor growth and metastasis, and antiangiogenesis is emerging as an effective strategy to treat human cancers.^{16,17}

Cisplatin is one of the cytotoxic drugs and is the most commonly used in the clinical context for tumor treatment for their broad-spectrum and curative effect. Cisplatin has been demonstrated to elicit antiangiogenic effects in solid tumors and has recently been shown to be effective against xenografts of lung cancer cells.¹⁸⁻²⁰ However, it also has serious side effects.

Endostar, an inhibitor of angiogenesis, is a modified recombinant human endostatin that is derived from rat vascular endothelial tumor cells and can inhibit endothelial cell proliferation and migration as well as apoptosis²¹⁻²⁴; therefore, endostar is thought to be an ideal anticancer weapon and is quickly pushed into clinical trials as well as used with concomitant chemoradiotherapy because of its favorable efficacy and tolerability profile. However, the response to this therapeutic regimen is variable.^{25,26} Previous studies have shown that the better response always bring a better prognosis than those with poor response.^{26,27} Long-term ineffective treatment not only brings great pain to patients but also increases their economic burden. Therefore, there is an urgent need to evaluate the effect of therapy in a timely manner.

Unfortunately, the quantity of residual viable tumor over the course of treatment is difficult to accurately assess because of limitations of conventional tools (X-ray, CT).²⁶

Molecular imaging can provide information about the changes of the tumor on the molecular level and quantify the amount of viable residual disease over the course of treatment. ^{99m}Tc-3PRGD₂ is a molecular imaging probe that has a positive correlation with the expression integrin $\alpha_v\beta_3$, because it utilizes a refined dimeric RGD peptide that has an enhanced binding affinity and improved tumor uptake as shown in preclinical experiments.²⁸⁻³¹ It is generally accepted that the T/N ratio of RGD-related imaging can reflect angiogenesis in tumors. Therefore, ^{99m}Tc-3PRGD₂ imaging can be used to predict treatment response indirectly by evaluating the angiogenesis status.

In this prospective study, the change of tumor volume between the treated group and NaCl group was significant ($P < .05$), and the change of endostar-treated group was much early than cisplatin-treated group. Additionally, significantly drop of the ^{99m}Tc-3PRGD₂ uptake in treated groups was showed. Moreover, between 2 treated groups, although the same final results have been achieved, the change of ^{99m}Tc-3PRGD₂ uptake in endostar-treated group was more evident than cisplatin-treated group from baseline after inoculation onward, suggesting that the inhibition effect of endostar was stronger than cisplatin. After consulting with oncologist, we think this result may be due to different pharmacological actions of endostar and cisplatin. Endostar can inhibit the formation of tumor newborn vascular and cause cytostatic effects, which mean a delay or stop of tumor progression during antiangiogenic treatment. It led to the decrease in integrin expression levels and corresponding targeted imaging probe uptake.

While cisplatin is a cytotoxic drug that leads to tumor cells disintegration based on the principle of tumor DNA damage. The eventual decrease in tumor angiogenesis is a result of volumetric change of tumor.

Our Western blotting and the imaging of ^{99m}Tc -3PRGD₂ uptake got the same trend. The integrin $\alpha_v\beta_3$ expression level of NaCl group was increasing from day 0 to 21, and the protein expression of day 21 answered the imaging result of day 21. On the contrary, the integrin $\alpha_v\beta_3$ expression level of the treated groups was more and more low from baseline to day 21, and it is proved by the protein bands of treated group; we could understand the change of T/N ratio shown as Figure 2B.

From analysis of the survival curve, we could learn that the tumor growth inhibition effect of treated groups was better than NaCl group. Furthermore, the tumor growth inhibition effect of endostar-treated group was better than cisplatin-treated group. The survival rate of endostar-treated group was much longer than cisplatin-treated group ($P < .05$). The results at individual level were in response to the results of tissue and protein level as mentioned above.

In summary, we demonstrated the ^{99m}Tc -3PRGD₂ enables the visualization and semiquantification of tumor angiogenesis in the xenograft model. Although it lacks histopathological information at early time points, by visualizing and measuring integrin $\alpha_v\beta_3$ expression on lung cancer cells and the vasculature, it can be concluded that ^{99m}Tc -3PRGD₂ could effectively monitor the response to the antiangiogenic therapy of endostar and cisplatin and predict the outcome of endostar and cisplatin therapy in xenograft animals.

Declaration of Conflicting Interests

The author(s) declared no potential conflicts of interest with respect to the research, authorship, and/or publication of this article.

Funding

The author(s) disclosed receipt of the following financial support for the research, authorship, and/or publication of this article: This work was supported by Norman Bethune Program of Jilin University (2015226 and 2015302), the Department of Education of Jilin Province for Thirteen-Five Scientific Technique Research (grant number: 2016461), Science and Technology Department Foundation of Jilin Province (20160101221JC, 20160204026YY), Jilin Province Development and Reform Commission Foundation (2017C046-4, 2019C052-8), and Youth Scientist and Technology Training Program/Health Commission of Jilin Province (2017Q008).

ORCID iD

Wei Sun  <https://orcid.org/0000-0003-0260-4484>

References

1. Torre LA, Bray F, Siegel RL, et al. Global cancer, statistics,2012. *CA Cancer J Clin.* 2015;65(2):87-108.
2. Ferrara N, Kerbel RS. Angiogenesis as a therapeutic target. *Nature.* 2005;438(7070):967-974.
3. Sheng J, Yang YP, Yang BJ, et al. Efficacy of addition of anti-angiogenic agents to taxanes-containing chemotherapy in advanced nonsmall-cell lung cancer: a meta-analysis and systematic review. *Medicine (Baltimore).* 2015;94(31):e1282.
4. Schreuder SM, Lensing R, Stoker J, Bipat S. Monitoring treatment response in patients undergoing chemoradiotherapy for locally advanced uterine cervical cancer by additional diffusion-weighted imaging: a systematic review. *J Magn Reson Imaging.* 2015;42(3):572-594.
5. Lange A, Prenzler A, Frank M, Golpon H, Welte T, von der Schulenburg JM. A systematic review of the cost-effectiveness of targeted therapies for metastatic non-small cell lung cancer (NSCLC). *BMC Pulm Med.* 2014;14(1):192.
6. Niu G, Chen X. Why integrin as a primary target for imaging and therapy. *Theranostics.* 2011;1:30-47.
7. Van Gool MH, Aukema TS, Hartemink KJ, Valdes Olmos RA, van Tinteren H, Klomp HM. FDG-PET/CT response evaluation during EGFR-TKI treatment in patients with NSCLC. *World J Radiol.* 2014;6(7):392-398.
8. Van Gool MH, Aukema TS, Schaake EE, et al. (18)F-fluorodeoxyglucose positron emission tomography versus computed tomography in predicting histopathological response to epidermal growth factor receptor-tyrosine kinase inhibitor treatment in resectable non-small cell lung cancer. *Ann Surg Oncol.* 2014;21(9):2831-2837.
9. Yang TJ, Aukema TS, van Tinteren H, Burgers S, Valdes Olmos R, Verheij M. Predicting early chemotherapy response with technetium-99m methoxyisobutylisonitrile SPECT/CT in advanced non-small cell lung cancer. *Mol Imaging Biol.* 2010;12(2):174-180.
10. Chen X, Sievers E, Hou Y, et al. Integrin alpha v beta 3-targeted imaging of lung cancer. *Neoplasia.* 2005;7(3):271-279.
11. Zhu Z, Miao W, Li Q, et al. ^{99m}Tc -3PRGD₂ for integrin receptor imaging of lung cancer: a multicenter study. *J Nucl Med.* 2012; 53(5):716-722.
12. Ma Q, Ji B, Jia B, et al. Differential diagnosis of solitary pulmonary nodules using (9)(9)mTc-3P(4)-RGD(2) scintigraphy. *Eur J Nucl Med Mol Imaging.* 2011;38(12):2145-2152.
13. Ji S, Zhou Y, Voorbach MJ, et al. Monitoring tumor response to linifanib therapy with SPECT/CT using the integrin alphavbeta3-targeted radiotracer ^{99m}Tc -3P-RGD2. *J Pharmacol Exp Ther.* 2013;346(2):251-258.
14. Ferrara N, Gerber HP. The role of vascular endothelial growth factor in angiogenesis. *Acta Haematol.* 2001;106(4):148-156.
15. Folkman J, Klagsbrun M. Angiogenic factors. *Science.* 1987; 235(4787):442-447.
16. Weidner N, Semple JP, Welch WR, Folkman J. Tumor angiogenesis and metastasis – correlation in invasive breast carcinoma. *N Engl J Med.* 1991;324(1):1-8.
17. Ferrara N, Hillan KJ, Gerber HP, Novotny W. Discovery and development of bevacizumab, an anti-VEGF antibody for treating cancer. *Nat Rev Drug Discov.* 2004;3(5):391-400.
18. Lee JG, Wu R. Erlotinib–cisplatin combination inhibits growth and angiogenesis through c-MYC and HIF-1 α in EGFR-mutated lung cancer in vitro and in vivo. *Neoplasia.* 2015;17(2):190-200.
19. Ma YP, Yang Y, Zhang S, et al. Efficient inhibition of lung cancer in murine model by plasmid-encoding VEGF short hairpin RNA in combination with low-dose DDP. *J Exp Clin Cancer Res.* 2010; 29(1):56.

20. Jiang QQ, Fan LY, Yang GL, et al. Improved therapeutic effectiveness by combining liposomal honokiol with cisplatin in lung cancer model. *BMC Cancer*. 2008;8(1):242.
21. O'Reilly MS, Boehm T, Shing Y, et al. Endostatin: an endogenous inhibitor of angiogenesis and tumor growth. *Cell*. 1997;88(2):277-285.
22. Dhanabal M, Volk R, Ramchandran R, et al. Cloning, expression, and in vitro activity of human endostatin. *Biochem Biophys Res Commun*. 1999;258(2):345-352.
23. Yamaguchi N, Anand-Apte B, Lee M, et al. Endostatin inhibits VEGF-induced endothelial cell migration and tumor growth independently of zinc binding. *EMBO J*. 1999;18(16):4414-4423.
24. Dhanabal M, Ramchandran R, Waterman MJ, et al. Endostatin induces endothelial cell apoptosis. *J Biol Chem*. 1999;274(17):11721-11726.
25. Dudek AZ, Mahaseth H. Circulating angiogenic cytokines in patients with advanced non-small cell lung cancer: correlation with treatment response and survival. *Cancer Invest*. 2005;23(3):193-200.
26. Huang W, Zhou T, Ma L, et al. Standard uptake value and metabolic tumor volume of (1)(8)F-FDG PET/CT predict short-term outcome early in the course of chemoradiotherapy in advanced non-small cell lung cancer. *Eur J Nucl Med Mol Imaging*. 2011;38(9):1628-1635.
27. Abdallah A, Belal M, El Bastawisy A, Gaafar R. Plasma vascular endothelial growth factor 165 in advanced non-small cell lung cancer. *Oncol Lett*. 2014;7(6):2121-2129.
28. Haubner R, Wester HJ, Weber WA, et al. Noninvasive imaging of alpha(v)beta3 integrin expression using ¹⁸F-labeled RGD-containing glycopeptide and positron emission tomography. *Cancer Res*. 2001;61(5):1781-1785.
29. Beer AJ, Haubner R, Goebel M, et al. Biodistribution and pharmacokinetics of the alphavbeta3-selective tracer ¹⁸F-galacto-RGD in cancer patients. *J Nucl Med*. 2005;46(8):1333-1341.
30. Kenny LM, Coombes RC, Oulie I, et al. Phase I trial of the positron-emitting Arg-Gly-Asp (RGD) peptide radioligand ¹⁸F-AH111585 in breast cancer patients. *J Nucl Med*. 2008;49(6):879-886.
31. Bach-Gansmo T, Danielsson R, Saracco A, et al. Integrin receptor imaging of breast cancer: a proof-of-concept study to evaluate ^{99m}Tc-NC100692. *J Nucl Med*. 2006;47(9):1434-1439.